The effects of laminar mixing on reaction fronts and patterns

I. Introduction

A wide variety of dynamical processes are influenced by some sort of reaction. In its most general sense, a "reaction" is when some species A changes into some other species B during a process, possibly via an interaction with other species. The most obvious example is a chemical reaction, when two or more reactants interact to form a third product, e.g., A + B → C or A + B → 2A. Combustion is an example of a chemical reaction, either in a controlled environment such as an engine or in an uncontrolled environment such as a forest fire. But reaction dynamics are found in other fields of science and engineering. In biology, for example, life cycle processes can be treated as reactions with different states when an animal is born, grows, and dies. Contraction of a disease can be treated as a reaction with at least two distinct states (healthy and sick). And various processes within living organisms can be treated as reactions; for example, waves of electrical activity in the heart are treated as reactions. Other examples of reactions include phase transitions where, for example, a solid (state "A") turns into a liquid ("B").

Reaction dynamics are heavily dependent on mixing in the system. For a chemical reaction in a flask, if the reactants are well-mixed, it can often be assumed that the reaction occurs everywhere in the system simultaneously. However, real systems are often spatially extended, and there are typically variations in concentration of the species in the system. The reactants need to be brought into proximity with each other to undergo a reaction; furthermore, the products of the reaction can interact with the remaining reactants. In the absence of any fluids flows, mixing is entirely via molecular diffusion. If there are fluid flows in the system, mixing is significantly enhanced over that due to molecular diffusion alone; consequently, fluid flows typically have a significant effect on the behavior of the system. If the flows are strongly turbulent, the mixing may be sufficiently strong such that the spatial extent of the system is not an issue (i.e., similar to a reaction in a well-stirred flask, the reaction occurs roughly simultaneously everywhere). However, it is often not possible to get strong enough turbulent mixing.

The strength of a fluid flow is typically characterized by the Reynolds number $Re = UL/\nu$, where U and L are the characteristic velocity and length scale of the flow and ν is the kinematic viscosity of the fluid. Turbulence requires a large Re, which is difficult for highly viscous flows or flows with a small characteristic length scale. The latter condition is particularly relevant for cellular-scale processes in biological organisms and for microfluidic devices, both of which have length scales that are often smaller than a micron. For small Re, the flow is laminar; in this situation, it is rarely the case that a reaction can be assumed to happen simultaneously throughout a system. In this case, the evolving reaction forms spatial patterns that are dependent on the combination of local reaction dynamics and longer-range mixing between different parts of the system.

The simplest type of spatially-extended, reacting systems are *reaction-diffusion* systems which, by definition, have no fluid flows. Mixing is entirely due to molecular diffusion, a process which is

inherently local in nature with each part of the fluid interacting only with the surrounding fluid. Reaction-diffusion systems have been studied extensively for several decades. For oscillating reactions (e.g., the oscillating Belousov-Zhabotinsky chemical reaction or life-cycle processes for living organisms) or for "excitable" reactions (one time reactions that can reset, such as the excitable Belousov-Zhabotinsky reaction, a disease from which someone can recover, electrical waves in the heart or brain, or a forest fire with trees that can re-grow), it is common for rotating spiral and expanding target patterns to form. For "one-off" ("burn-type") reactions that do not reset (e.g., combustion of a fuel, solidification of a cooling melt, or the propagation of a deadly disease), it is typical for fronts to develop which propagate across the system with a well-defined front velocity that depends on the molecular diffusivity and reaction rates of the interacting species.

The addition of a fluid flow dramatically changes the pattern-formation and front propagation behavior[1]. This is relevant to a wide range of reacting systems, including ecosystems in oceanic flows, forest fires in the presence of wind, and chemical and biological processing systems that are subject to fluid flows. There has been a significant amount of previous research into the effects of *turbulent* flows on reaction dynamics (e.g., in turbines and in pre-mixed burners). Surprisingly, however, there has not been much research until recently on the effects of *laminar* fluid flows on reaction dynamics. Laminar flows are relevant for a wide range of reacting systems, including micro-fluidic reactors (so called "laboratories on a chip") and biological processes in cellular and embryonic systems, all of which occur on small enough scales such that Reynolds numbers are too small to sustain turbulent flows.

This chapter discusses recent research on the effects of laminar fluid mixing on reaction dynamics. We review both theoretical and experimental studies, and discuss areas that are currently being studied and for which significant additional research is needed. In Section II, we present background material on relevant issues in fluid mixing, along with previous results in reaction-diffusion systems. Section III covers some of the basic principles common to *advection-reaction-diffusion* (ARD) systems, i.e., reacting systems with fluid mixing. Section IV discusses recent studies that examine how laminar fluid mixing affects local pattern formation in ARD systems. Section V discusses synchronization of processes in extended fluid systems and how laminar mixing relates to that synchronization. Section VI discusses the issue of front propagation and how laminar mixing affects the process. Section VII summarizes and discusses future areas of investigation.

II. Background

A. Laminar mixing – the Advection-Diffusion Equation

Mixing is governed by the interplay between advection of impurities along streamlines as they are carried by a fluid flow and diffusion of the impurities between streamlines in the flow. Quantitatively, the process is governed by the advection-diffusion equation (also known as the *convection-diffusion equation*):

$$\partial c / \partial t + \vec{v} \bullet \vec{\nabla} c = D \nabla^2 c ,$$

where $c(\vec{r}, t)$ is the concentration field for the impurity, $\vec{v}(\vec{r}, t)$ is the velocity field, and *D* is the molecular diffusion coefficient for the impurity in the background fluid. Conceptually, the concentration of the impurity at a location changes either if the flow carries a region of lower or higher concentration to the point of interest, or if there is diffusion of impurity into our out of the point of interest from the neighboring regions. In non-dimensional form, the advection-diffusion equation is written as

$$\partial c / \partial t = \tfrac{1}{Pe} \nabla^2 c - \vec{v} \bullet \vec{\nabla} c ,$$

where all the quantities have been non-dimensionalized by the characteristic velocity *U* and length *L* scales of the flow, and the *Peclet number* is defined as *Pe = UL/D*. Conceptually, the Peclet number characterizes the relative strength of the advection and diffusion terms. Mixing with $Pe \gg 1$ is dominated by advection, whereas $Pe \ll 1$ corresponds to diffusion-dominated mixing.

B. Short-range mixing

Several techniques have been developed to characterize local mixing in fluid flows. Many of these techniques involve quantification of the manner in which the flow stretches fluid elements. Quantitatively, stretching is characterized by a positive finite-time Lyapunov exponent (FTLE) λ(t) defined by:

$$\lambda(t) = \frac{1}{t} \ln\left(\frac{\Delta r(t)}{\Delta r_0} \right),$$

where $\Delta r(t)$ is the separation of two passive tracers after a time *t*, and Δr_0 is the initial separation of those two tracers (assumed to be much smaller than typical length scales of the flow). If mixing is chaotic, then a positive Lyapunov exponent can be found even in the infinite-time limit. The FTLE can be represented as a field, showing visually the regions of maximal stretching in a flow.

Stretching of fluid elements in itself is not the prime contributor to mixing; rather, compression of streaks of impurity is the key. However, since most laminar flows are incompressible, significant stretching of fluid elements (and large positive Lyapunov exponents) is associated with significant compression of the same fluid elements in an orthogonal direction, characterized by large negative Lyapunov exponents. Compression of fluid elements results in thinning of tendrils of impurity in the flow. Ultimately, complete mixing occurs as a two-stage process: advection of the impurity in the flow stretches (and thins) and folds the impurity repeatedly until the structures are thin enough so that molecular diffusion can finish the job.

Recently, there has been a tremendous interest in what are referred to as *Lagrangian Coherent Structures* (LCS) as a method for identifying regions of significant mixing in a fluid flow. These structures are equivalent to *unstable manifolds* of fixed points in a fluid flow, as shown in Figure 1. The unstable manifold of a fixed point is defined as the future location of a swarm of tracer particles that start out infinitesimally close to the fixed point. For a time-independent flow (Fig. 1a), the unstable manifold of a fixed point is usually a simple curve that separates different mixing regions in the flow; i.e., it is frequently equivalent to the separatrix. If the flow is time-periodic (Fig. 1b), the manifold undulates, forming a pattern of folds that become increasingly complicated in time and distance from the fixed point. A stable manifold can also be defined for a fixed point, either as the set of points that in the distant future will end up arbitrarily close to the fixed point, or as the set up points which would denote the unstable manifold of that fixed point of time were reversed.

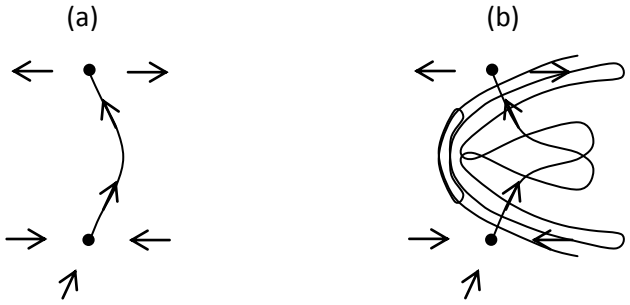

Figure 1. Stable and unstable manifolds of two hyperbolic fixed points in a flow. (a) Time-independent flow; the unstable manifold of the lower fixed point is the same as the stable manifold of the upper fixed point. (b) Time-periodic flow; the unstable manifold of the bottom fixed point undulates, as does the stable manifold of the upper fixed point.

From a perspective of short-range mixing, the unstable manifold is the region of the flow where stretching is maximized; consequently, compression in the orthogonal direction is also maximized and mixing is strong and efficient. These manifold techniques were pioneered a couple of decades ago for

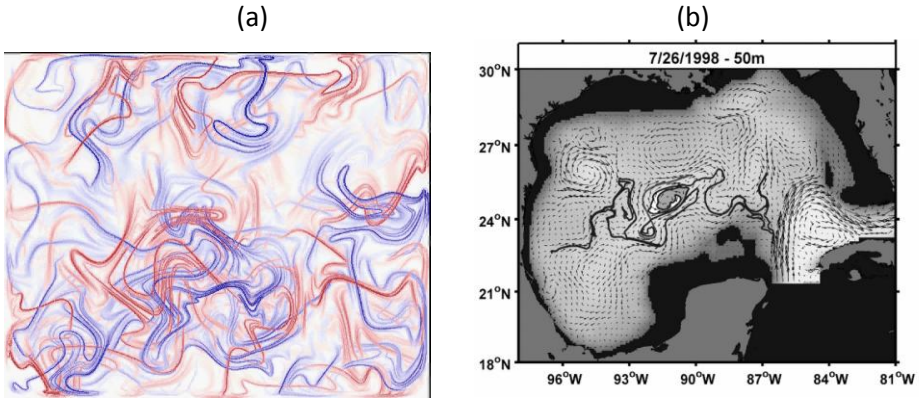

Figure 2. Stable and unstable manifolds in more complicated flows. (a) Manifolds from weakly turbulent magnetically-forced flow (from Greg Voth and Jerry Gollub; see Ref. 2). (b) Manifolds and hyperbolic trajectory of Eddy Fourchon in the Gulf of Mexico (from Ref. 3).

time independent and time-periodic flows. Recently, research groups have successfully extended these ideas to enable the experimental identification of both stable unstable manifolds to turbulent fluid flows[2] (Figure 2a). These approaches have been used very successful to analyze mixing in flows in the oceans and in the Gulf of Mexico.[3,4]

C. Long-range transport of impurities

Stable and unstable manifolds can also be used to quantify long-range transport in extended fluid flows; specifically, over distances larger than characteristic length scales in the flow. A paradigmatic flow for these studies is the alternating vortex chain (Figure 3), a flow that is common in nature, e.g., in flows

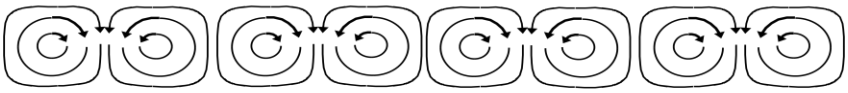

Figure 3. Sketch of alternating vortex chain. In the studies presented in this chapter, the vortex chain can move laterally, either oscillating periodically with a maximum lateral speed v_o, moving with a constant drift velocity v_d, or moving with a combination of oscillatory and drifting motion.

with thermal convection, sheared flows, and cloud streets. If we approximate the flow as two-dimensional (2D) or consider a 2D cross-section of a 3D flow, each vortex is a separate mixing region, and long-range transport is achieved only if there is a mechanism for tracers to cross the separatrices between adjacent vortices. For a time-independent flow, the separatrices are manifolds for the fixed points at the vortex corners, and transport between vortices occurs only via molecular diffusion of impurity across these separatrices. If the flow is time-periodic, however, the folded stable and unstable manifolds intersect to form a pattern of lobes (Figure 4) that provides an advective mechanism that enables impurities to cross from one vortex to the next. In Figure 4, impurities in the bottom filled-in lobe end up in the next lobe (above the first and to the left of the separatrix) one period later, then the

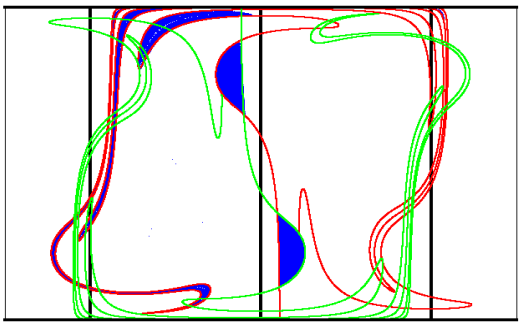

Figure 4: Stable and unstable manifolds of the hyperbolic fixed points for the alternating vortex chain. The straight vertical lines are the separatrices between adjacent vortices, and are also the manifolds for the time-independent case with no lateral oscillations. The complicated (stretched and folded) manifolds correspond to time-periodic, lateral oscillations of the vortex chain. Some of the lobes formed from the intersections of these manifolds are shaded in.

next lobe (near the top) one period after that, etc. Similarly, impurities in the bottom, clear lobe end up in the middle lobe (straddling the separatrix) one period later, then the top, clear lobe, etc. This "turnstile" mechanism results in transport of impurities between adjacent vortices, with the amount being transported being determined by the area of the lobes.

To first order, this lobe mechanism of transport results in long-range transport that is essentially diffusive with an impurity distribution whose variance grows linearly in time: $< x^2(t) >= 2D^* t$, where D^* is the effective (enhanced) diffusion coefficient. Experiments have been done[5,6] to test these ideas quantitatively; the results of the experiments verify this lobe picture of long-range transport, along with the typically-diffusive nature of the transport.

Long-range transport in an advection-diffusion system is not necessarily diffusive. More generally, the variance grows as a power law in time: $< x^2(t) > \sim t^{\gamma}$. If $\gamma = 1$, then the transport is diffusive. If $\gamma \neq 1$, then the transport is deemed "anomalous" with $\gamma < 1$ corresponding to *subdiffusive* transport and $\gamma > 1$ corresponding to *superdiffusive* transport. Superdiffusive transport is associated with trajectories called *Lévy flights*[7,8,9] where tracers in the flow undergo sporadic "jumps" whose lengths follow a power-law probability distribution: $P(L) \sim L^{-\mu}$, where $\mu < 3$. This is a probability distribution whose second moment diverges: $<L^2> = \infty$. Lévy flights and superdiffusion were first seen experimentally in a chain of time-periodic *co-rotating* vortices[10], but they can also be found in the time-periodic counter-rotating vortex chain if either the oscillation frequency is resonant with a typical circulation time[11] or if a uniform wind is added to the flow[12] with velocity magnitude $W > v_{osc}$, where v_{osc} is the maximum lateral oscillation velocity of the vortex chain.

Since the first experiments in the early 1990s that showed Lévy flights and superdiffusion, Lévy flights have been discussed for a wide range of systems, including the motion of people in society[13] and the foraging patterns of various animals[14,15]. Consequently, superdiffusion is most likely relevant to a range of real systems.

D. Nonlinear reactions

In the mid-1950s, Boris Belousov discovered a chemical reaction that approaches equilibrium in a long, cyclical process in which the pH of the solution oscillates for up to several hours. When tagged with an indicator, the solution changes color, alternating between two different colors through the life of the reaction. The same effect was rediscovered a few years later by Anatol Zhabotinsky. The reaction and its variants – where are now referred to broadly as the *Belousov-Zhabotinsky* (BZ) reaction – has been studied extensively for the past few decades as a paradigm for nonlinear reactions[16,17,18].

Two different regimes are common for BZ and similar reactions, depending on the relative concentrations of the reactants: (a) an oscillatory regime in which the pH spontaneously oscillates periodically (or almost periodically) for many oscillation periods before the reaction finally reaches

equilibrium; and (b) an excitable regime in which the reaction requires some sort of trigger to change its pH (and its color if an indicator is used), but then returns to its initial pH and color.

The BZ reaction has also been manipulated to produce chaotic time dependence, if configured in a continuously-stirred tank reactor (CSTR) where new chemical reactants are continuously fed into the system.

E. Reaction-diffusion systems

When nonlinear reactions are in an extended system, the interaction between local reaction dynamics and diffusive mixing results in a variety of spatial patterns and front-producing behavior. In the absence of a fluid flow, these systems are referred to generally as *reaction-diffusion* (RD) systems, described generically by the reaction-diffusion equation:

$$\partial c_i / \partial t = D_i \nabla^2 c_i + f_i(c_1, c_2, c_3, ...) .$$

Here, c_i is the concentration of one of the species in the system, D_i is the molecular diffusion coefficient for that species and f_i is the reaction term, which depends not only on c_i but also on the other species in the system.

The behavior of fronts moving in a reaction-diffusion system has been well studied for reactions that are described[19,20] by a complex function *f(c)* where *f'' < 0*. In this case, the front propagates with a speed $v_{rd} = \sqrt{2D/\tau_r}$ where *D* is the molecular diffusion coefficient for the relevant reactants and τ_r is the time scale for the reaction. This theory – referred to as *FKPP* theory since it was developed separately by Fisher[21] and by Kolmogorov, Petrovsky and Piskunov[22] – is well-established, and applies to a wide range of reacting systems, not only chemical but biological and physical as well, as long as a diffusivity and reaction time scale can be identified.

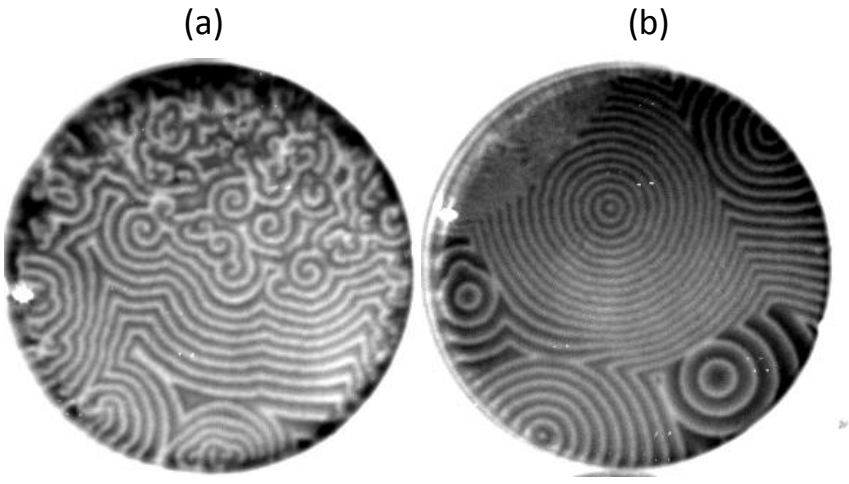

Figure 5. (a) Spiral and (b) target patterns in the excitable Belousov-Zhabotinsky chemical reaction in a Petri dish with no imposed fluid flow.

Reaction-diffusion systems are also well-known for their ability to form patterns[16]. The Belousov-Zhabotinsky (BZ) reaction in its excitable regime readily forms patterns composed of target and spiral patterns, as shown in Figure 5. Conceptually, these patterns – referred to as *trigger waves* – form due to the ability of a triggered excitable reaction to reset back to (roughly) its original state, after which it can be retriggered. A rotating spiral is an example of a self-sustaining pattern for an excitable system. This kind of self-sustaining pattern formation behavior appears even if the reaction is oscillatory. Initially, the entire reaction oscillates together, but over time, the oscillations de-synchronize, forming regions of *phase waves*. In some of these regions, seeds of trigger waves form, and these trigger waves grow in extent into the phase wave regions.

Pattern formation in the BZ chemical reaction in the RD limit has been studied extensively, predominately because the behavior seen in this system is typical of pattern formation seen in a wide range of RD systems. Examples – shown in Figure 6 – include waves of electrical activity in the heart[23] which are responsible for the heart's pace-maker, *spreading depression* in the visual cortex[24] which is responsible for the visual patterns seen in migraine headaches, and patterns formed in slime mold cultures[25] (*Dictyostelium discoideum*).

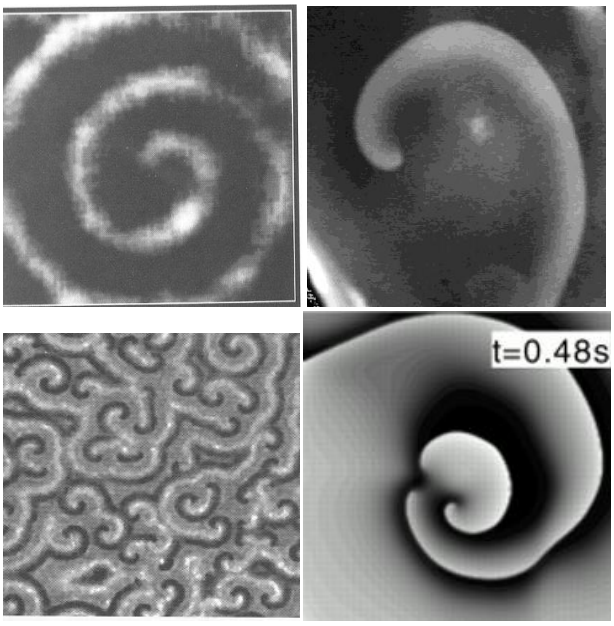

Figure 6: Reaction-diffusion patterns in other systems. Upper-left: developing frog embryos (David Clapham, May Foundation). Upper-right: spreading depression in the visual cortex (Stefan Muller, Univ. Magdeburg). Lower-left: slime mold cultures (Cornelis Weijer, Univ. Dundee). Lower-right: electrical waves in heart (Qu, Weiss and Garfinkel)

III. Advection-Reaction-Diffusion: General Principles

When there is both a reaction and a fluid flow, the system can be described in general by the advection-reaction-diffusion (ARD) equation:

$$\partial c_i / \partial t = -\vec{v} \bullet \vec{\nabla} c_i + D_i \nabla^2 c_i + f_i(c_1, c_2, c_3, \ldots),$$

which combines the advection-diffusion and reaction-diffusion equations. Conceptually, this equation states simply that the concentration of a species at a location changes due to, respectively, advection of that species from other locations due to a fluid flow ($-\vec{v} \bullet \vec{\nabla} c_i$), diffusion to and from neighboring regions ($D_i \nabla^2 c_i$) and reaction of c_i with other species that can change the concentration locally ($f_i(c_1, c_2, c_3, \ldots)$). Written in non-dimensional form[26], the ARD equation becomes:

$$\partial c_i / \partial t = -\vec{v} \bullet \vec{\nabla} c_i + Pe^{-1} \nabla^2 c_i + Da \cdot f_i(c_1, c_2, c_3, \ldots),$$

where we have introduced the *Damkohler number* $Da = L/U\tau_r$. The Damkohler number can be written as the ratio of the advective time scale τ_a to the reaction time scale τ_r: $Da = \tau_a/\tau_r$; consequently, a large *Da* corresponds to an ARD system in which the flow doesn't move the reactive species very far during a typical reaction time, whereas a small *Da* corresponds to an ARD system in which the reactive species are mixed significantly during typical reaction times.

The Damkohler number does not, however, take into account the role of diffusion in the ARD process, and the Peclet number (which weighs the relative strengths of advection and diffusion) does not account for the reaction. Another dimensionless number[27] that is appropriate for front behavior in ARD systems can be defined by the ratio of the characteristic advective velocity *U* to the speed v_{rd} at which a front propagates in the reaction-diffusion limit (i.e., U → 0): $\mu = U/v_{rd}$.

There have been numerous studies of ARD systems with turbulent flows; in particular, the problem of turbulent combustion has received a lot of attention due to its clear applications in various fields of engineering. However, the behavior of ARD systems in laminar flows has only recently received attention, most of which is theoretical.

IV. Local Behavior of ARD Systems

The tools used to describe chaotic mixing have been used successfully to characterize the patterns that form in ARD systems. Locally, chemical patterns tend to follow the mixing structures in the flow. Experiments in the early 1990s[28] measured regions of maximum chemical activity in one-time reactions and found that these regions matched up well with the regions of maximum stretching of impurities in the flow. More recent experiments in magnetically-driven vortex flows[29] also used stretching fields to characterize regions of significant chemical activity in one-time reactions.

The use of stretching fields to characterize chemical activity makes sense, considering that the regions where fluid elements are most significantly stretched are also regions of maximal compression in orthogonal directions and are therefore regions where molecular diffusion can mix impurities most efficiently. Note that this is effectively equivalent to using fields of finite time Lyapunov exponents, which is effectively the logarithm of the stretching field, normalized by the time span.

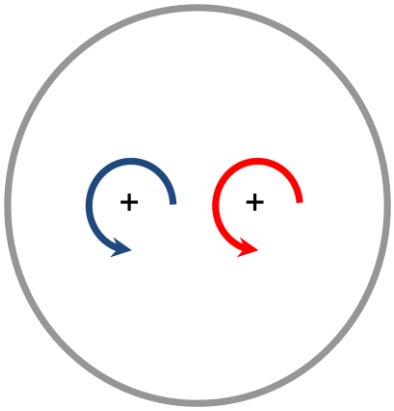

Figure 7: Blinking vortex flow. The flow has periodic time-dependence. During half of the period, fluid circulates around the left point vortex; during the other half of the period, fluid circulates around the right point vortex. The flow continues to "blink" periodically between these two vortices. The source-sink version of this flow has sources and sinks of fluid at the vortex centers.

Theoretical studies[1] during the first decade in the 2000's described this phenomenon in terms of unstable manifolds of fixed points in the flow. Theory and modeling have been done for burn-type reactions in a blinking vortex flow (Figure 7) with source and sink terms. Mixing in this flow is chaotic, similar to that in Hassan Aref's original blinking vortex flow model of 1984, but the addition of a source and sink makes this an "open" flow in which the reactants are replenished. So, instead of the region of "burned" reactants growing indefinitely until it covers the entire system, there is ultimately a balance condition and a steady-state pattern forms around the unstable manifolds of the flow (Figure 8).

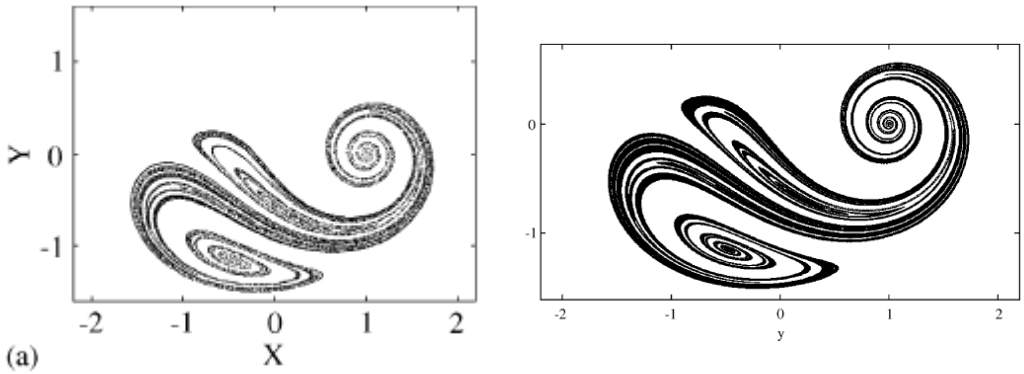

Figure 8: Numerical unstable manifold (left) and pattern for autocatalytic reaction (right) for blinking vortex-sink system. (T. Tél et al, Ref. 1)

Similar behavior is observed for "closed" flows with oscillating reactions[30]. Since the reaction oscillates rather than burning across the entire system, it isn't necessary to replenish the reactants to avoid having the burned front growing in area indefinitely. Experiments were done in a blinking vortex flow (without sources and sinks) and the patterns that formed in these experiments agreed very well with patterns obtained from *mixing fields* of the flow which are basically stretching fields but chosen with a timescale equal to the time for the BZ pattern to decorrelate in the absence of any fluid flows. Examples from these experiments are shown in Figure 9.

(a) (b)

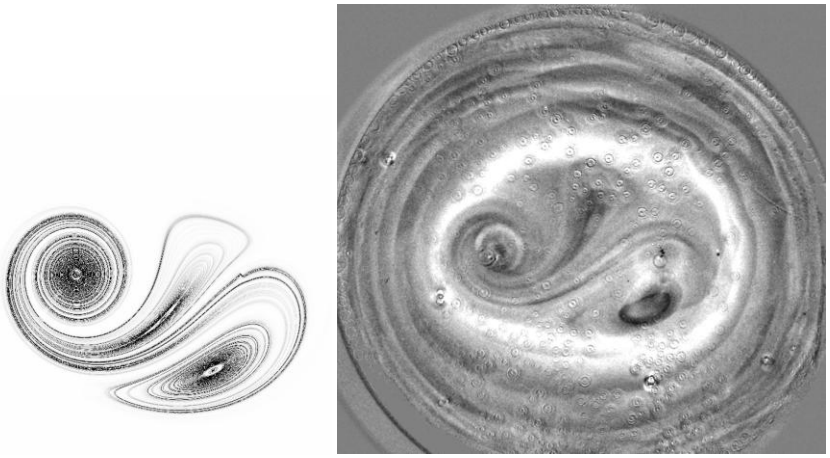

Figure 9: (a) Mixing field for blinking vortex flow. (b) Pattern formed by oscillating Belousov-Zhabotinsky reaction in blinking vortex flow (Ref. 30)

Finally, the behavior discussed in this section for chemical reactions in both open and closed flows applies to other, non-chemical systems. In particular, several studies[31,32] have investigated "blooms" of algae and phytoplankton in the oceans and Gulf of Mexico, using the same analytical techniques involving manifolds for mixing in these bodies of water.

Another issue involving local pattern formation in ARD systems is that of *extinction*; i.e., when the mixing is strong enough so that the reaction is terminated (like a flame being blown out). In fact, some reactions are bistable where the reaction either spreads and eventually covers the entire system (space-filling) or is completely extinguished by the flow.[33]

V. Synchronization of Oscillating Reactions

In a fluid system, mixing is the key to understanding when time-varying processes synchronize. In the studies of pattern formation for oscillating reactions discussed in the previous section, the thickness of the oscillating structures increase with the mixing efficiency of the flow. In the limit of perfect mixing, the thickness of the structures diverges to the length of the entire system; in this limit, the reaction is synchronized throughout the system.

A few studies have investigated how mixing contributes to synchronization in fluid networks, where individual nodes can be identified and where the mixing between these nodes is controlled. In one series of studies[34], the chaotic mixing in the system is analyzed theoretically as a global coupling between the different oscillators. Regimes of complete synchronization are found, as well as regimes of "oscillator death" when the coupling due to mixing ends the reaction entirely (similar to extinction, discussed in the previous section).

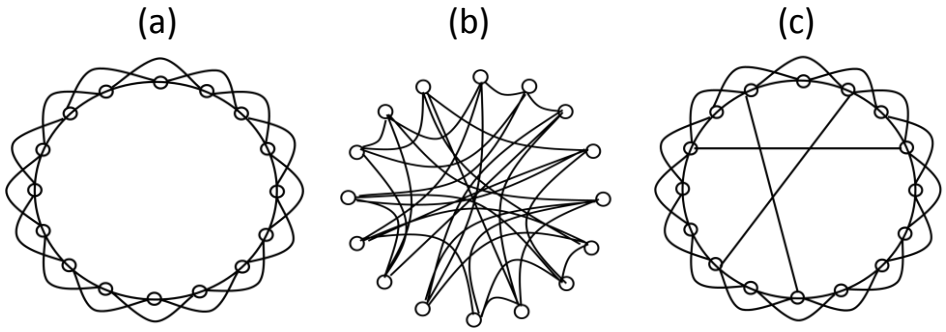

Figure 10: Different models for connected networks. (a) Nearest-neighbor model where each node of the network is connected with its two nearest neighbords. (b) Random model where nodes are connected in a random pattern. (c) "Small-World" network which is predominately a nearest-neighbor model, but with a few, long-distance "short-cut" connections.

Experiments have been done on coupling of individual oscillators. In one study[35], an array of up to 64 Ni electrodes was immersed in an electrochemical apparatus. Coupling in this experiment is achieved electronically, however, rather than via fluid mixing. These experiments demonstrated that sufficient coupling could lead to global synchronization or oscillator death, depending on the circumstances.

In an extended system, the type of long-range transport affects the manner in which different parts of the system are coupled. As discussed in Section II.C., diffusive transport is associated with fluid elements that undergo random-like walks between neighboring regions in the flow, whereas superdiffusive transport is associated with Lévy flight trajectories where fluid elements can travel large distances in a short period of time. From a network perspective, a system with diffusive transport is akin to a network with nearest-neighbor coupling (Figure 10a) whereas a system with superdiffusive transport is analogous to a network with long-range connections (Figure 10c). This is reminiscent of the studies done at the end of the 1990's on network models and, in particular, on the small-world network models[36] that use long-range "short-cut" connections to enhance dramatically the connectivity of a network.

Two experimental programs have studied the effects of different types of long-range transport on the behavior of a network of chemical oscillators. In one study[37], instead of using a fluid flow, the long-range "transport" is simulated experimentally by using a photo-sensitive (Ruthenium-catalyzed) version of the BZ reaction and a feedback mechanism using imaging and an LCD projector. Long-distance coupling is achieved by measuring fluctuations in the reaction at a particular location and then adjusting the projector intensity at another location in response to that fluctuation. If the long-range feedback is implemented with a power-law relation (i.e., describing coupling amplitude versus distance, similar to Lévy flights) then long-range synchronization of the reaction dynamics is found.

Another concurrent study[12] studied the effects of fluid mixing on long-range synchronization more directly. The flow studied was the oscillating/drifting vortex chain described in Section II.C and shown in Figure 3. The fluid is composed of the chemicals for the BZ reaction, and each vortex acts as an individual chemical oscillator that is coupled to other nodes in the network via fluid mixing. In the absence of any oscillation or drift of the vortices, each vortex is essentially isolated from its neighbors except via molecular diffusion; consequently, the BZ oscillations occurring within the vortices become complete desynchronized. If there is lateral motion of the vortices and if the drift velocity (equivalent to the speed of an imposed wind in a co-drifting reference frame) v_d is less than the maximum lateral oscillation speed v_o of the vortices, then the transport is diffusive and the coupling is effectively nearest-neighbor. In this situation, the system spontaneously forms traveling phase waves with a complicated (possibly chaotic) time evolution (Figure 11a). On the other hand, if $v_d > v_o$, the transport is superdiffusive (with Lévy flights) and there is significant long-range coupling between the reactions oscillating within the vortices (Figure 11b and c). In this situation, the oscillations within the vortices rapidly synchronize globally. The result is clear: the type of long-range fluid mixing has a significant effect on collective behavior of a fluid network of oscillating reactions.

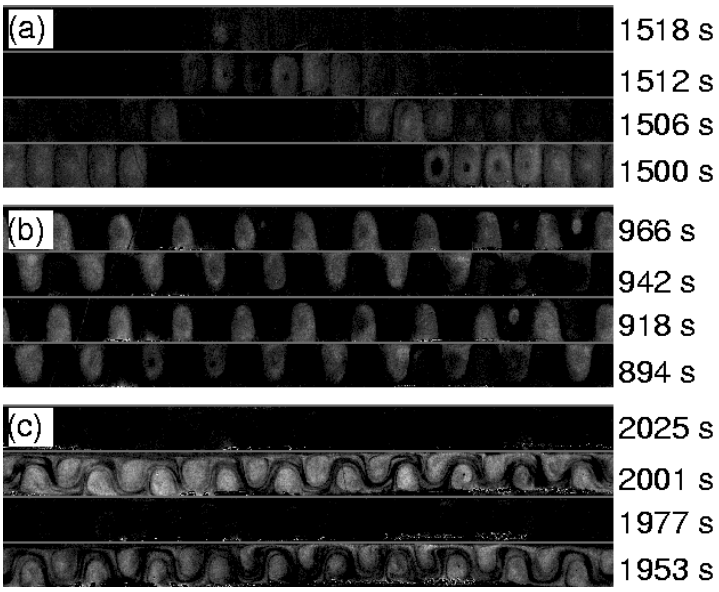

Figure 11: Sequences of images of oscillating BZ reaction in an annular chain of oscillating/drifting vortices. The annulus has been "de-curled" to show the vortices in a strip. (a) Periodic lateral oscillations. Traveling waves form that propagate around the annulus in an unpredictable manner. (b) Periodic lateral oscillations with a superposed DC drift; mixing is superdiffusive, coupling every second vortex. Oscillations of the BZ reaction in the vortices synchronize in alternating (odd or even) vortices. (c) Oscillating/drifting time dependence with superdiffusive mixing that connects all the vortices. The BZ oscillations are globally synchronized. (From Ref. 12)

The issue of the effects of fluid mixing on synchronization is still a very open issue with many unanswered questions. Theoretical modeling of the drifting/oscillating vortex chain experiments has not been done yet. There are differences between the simple Watt/Strogatz small-world network model[36] and the coupling due to superdiffusion and Lévy flights in an extended fluid system. First, coupling due to superdiffusion isn't only between random vortices; rather, every vortex is coupled to every other vortex in the system with a coupling strength that decays as a power law with distance. Second, the duration of the flights has to be taken into account; fluid elements in a flight take a finite time to complete the excursion, and if that time exceeds typical correlation times for the reaction, that could affect the ability of superdiffusion to synchronize an extended fluid network.

Another open question is how applicable these ideas are to a range of oscillating systems occurring either in fluid flows or as part of a "flowing" system. For instance, networks of people in a moving population may be considered – for a sufficiently large number of people – as a flow, in which case it might be instructive to model dynamical processes affecting moving populations as a continuous advection-reaction-diffusion system.

VI. Front Propagation in Advection-Reaction-Diffusion Systems

There have been very few theoretical studies of how front propagation is affected by the presence of a fluid flow. In the case where the enhanced transport is diffusive, the problem for front propagation seems almost obvious: simply take the FKPP prediction $v_{rd} = \sqrt{2D/\tau_r}$ and replace the molecular diffusion coefficient with the enhanced diffusivity D^* describing transport in the flow. However, as we discuss below, there are experiments for which this approach clearly does not work. There have been several theoretical studies that extend FKPP theory to cases with superdiffusive transport[38], most using techniques derived from fractional calculus, which is a mathematical language that is well-suited for incorporating long-distance interactions produced by Lévy flights. However, the fact that an FKPP approach does not adequately describe front propagation in ARD systems with enhanced diffusion raises questions about whether a modified version of FKPP theory will work for superdiffusive cases. (Experimental data for the superdiffusive case is still lacking.)

The main issue when dealing with front propagation in ARD systems appears to be the role of coherent flow structures on the front propagation phenomena. In particular, vortices play a significant role in the process beyond the role expected simply by their effect on the enhanced diffusivity. The first indications of difficulties with an FKPP approach to front propagation in ARD systems was provided by a series of numerical studies[19,20] and experimental studies[39] that studied front propagation in the oscillating vortex chain flow discussed in Section II.C (Figure 3). Numerical and experimental sequences of images of a front in this flow are shown in Figure 12. The fronts are observed to *mode-lock* to the external, time-periodic, lateral oscillations of the vortex chain, moving an integer number N of unit cells λ of the flow (where one unit cell λ is two vortex widths) in an integer number M of oscillation periods. Figure 12(a) and (b) show an example of (N,M) = (1,1) mode-locking where the front moves 1 unit cell (two vortex widths) each drive period, and Figure 12 (c) and (d) shows an example with (1,2) mode-locking where the front moves 1 unit cell in 2 drive periods (and 1 vortex every period, although the front flips each period).

The front velocity when mode-locked depends on the combination (N,M), the vortex width and the drive period T or frequency f: $v_f = (N\lambda)/(MT) = (N/M)\lambda f$. The (enhanced) diffusivity of the chemical species and the reaction time scales do not directly affect the front propagation speed. A plot of experimental front speeds is shown in Figure 13, along with the predictions for mode-locked fronts. There are no

fitted parameters in this figure – the experimental data agree almost perfectly with the mode-locking predictions.

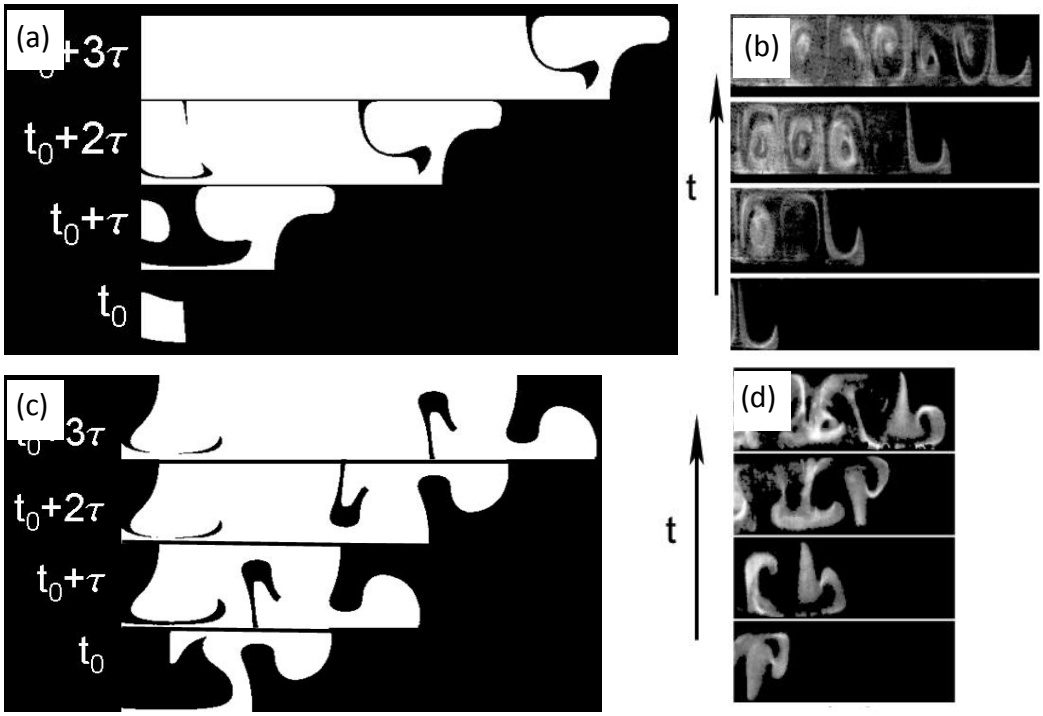

Figure 12: Mode-locking for front propagation in an oscillating chain of vortices. (a) Simulation and (b) experiments showing (1,1) mode-locking where the front moves 1 wavelength (2 vortices) each drive period. (c) Simulation and (d) experiments showing (1,2) mode-locking where the front moves 1 wavelength in 2 drive periods (or 1 vortex every period).

The horizontal line in Fig. 13 shows the front speed in the absence of any lateral oscillations of the vortex chain. The fact that some of the front speeds with the time-periodic oscillations are actually *slower* than the front speed for the time-independent flow is the clearest evidence of the inapplicability of an enhanced-FKPP approach, since the effective diffusivity for any time-periodic flow (with lateral oscillations of the vortex chain) is significantly larger than that for the time-independent case (no lateral oscillations), so a larger front speed would be expected from an FKPP approach based on the enhanced diffusivity.

The key appears to be the behavior of a reaction front when it encounters a vortex in the flow, especially if the vortex is moving. Experimental studies[27] have demonstrated that moving vortices pin and drag reaction fronts. Alternately, in a reference frame that is co-moving with the vortices, the reaction front is "frozen" in the leading vortex in the face of an imposed wind, as shown in Figure 14. This behavior is seen not just for an ordered chain of vortices but also for random, vortex-dominated flows. Recent studies of the behavior of phytoplankton blooms in oceanic vortex flows[40] have also demonstrated the ability of moving vortices to pin and drag reacting species.

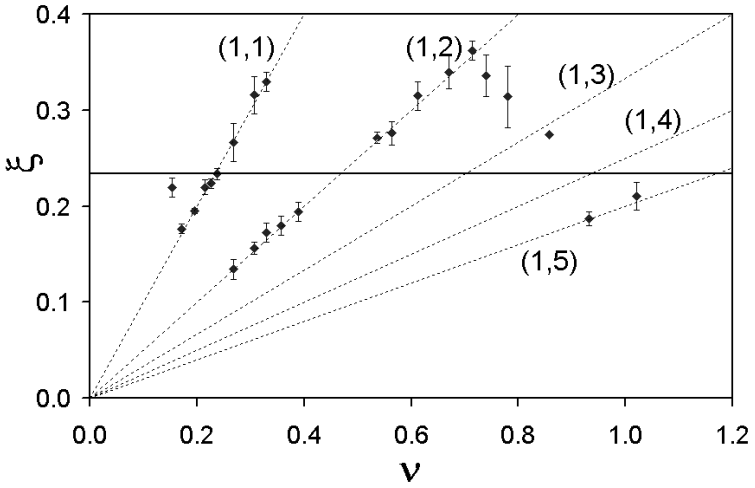

Figure 13: Experimentally-determined reaction front velocities in oscillating vortex chain. The front velocities ξ are non-dimensionalized by the maximum flow velocity *U,* and the frequency ν of oscillation is non-dimensionalized by *U* and by the vortex width $d = \lambda/2$. The diagonal lines are the front speeds predicted for mode-locking (From Ref. 39)

Ultimately, a general theory of front propagation in ARD systems is needed in which the role of coherent flow structures is taken into accounted. Studies are on-going about the possibility of a general approach based on pinning of fronts on vortices. Another approach being pursued is to try to extend the approaches used to describe chaotic fluid mixing to account for front propagation phenomena. In particular, it might be possible to extend manifold/lobe approach discussed in Sections II.B and C – that describes the motion of passive impurities in a flow – to account for the motion of a front in a flow, which moves by a combination of advection and reactive spreading.

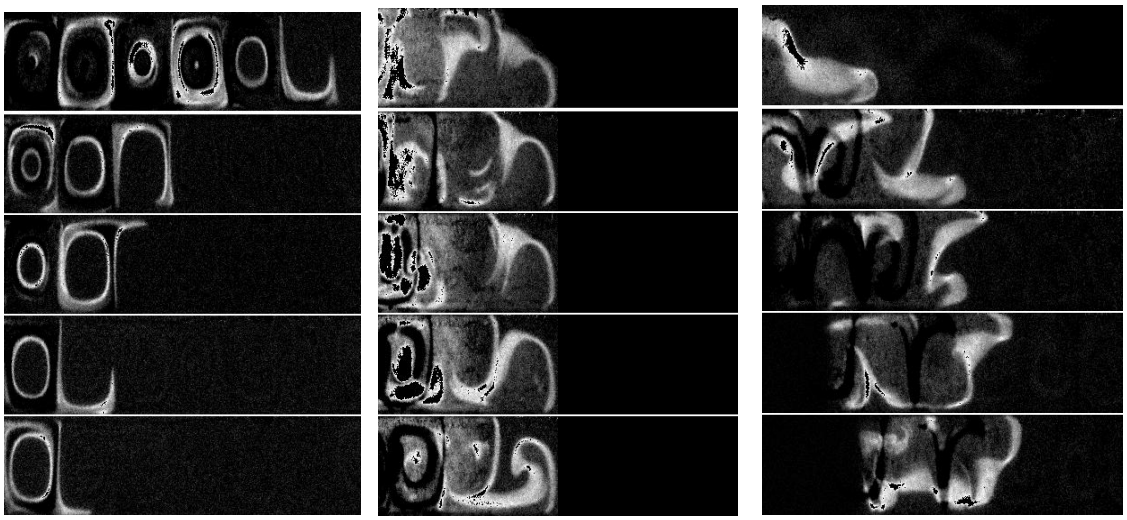

Figure 14: Reaction fronts in the presence of a leftward-directed wind imposed on the vortex chain. Time increases going upward in these sequences. If the wind speed *W* is smaller than the reaction-diffusion front speed v_{rd} (left sequence), then the front propagates to the right against the wind. For moderate wind speeds ($v_{rd} < W$, but *W* can be several times – and more than an order of magnitude – greater than v_{rd}), as in the middle dequence, the front remains "frozen" to the leading vortex, propagating neither forward nor backward. For large enough wind speeds (right sequence), the front is blown backwards against the wind. (From Ref **Error! Bookmark not defined.**)

The bottom line: a general theory to describe front propagation in advection-reaction-diffusion systems is still needed.

VII. Additional Comments

The field of advection-reaction-diffusion for laminar fluid flows is still in its infancy. This is a field with a significant range of applications over a wide range of fields in science and engineering. At the smallest scales, laminar ARD behavior is relevant for micro-fluidic devices for which large Reynolds numbers are unachievable. Similarly, biological processes on a cellular or embryonic scale can be cast as ARD systems with laminar fluid flows. At everyday scales, an ARD analysis might shed light on plasma processes and might help in the development of safe nuclear fusion technologies. At larger scales, ARD phenomena have already been observed and explained for ecosystems in oceanic-scale flows. It has even been proposed that the motion of ignition fronts within a star during a supernova explosion might be modeled as an ARD phenomenon.

Finally, it is possible that even discrete systems can be modeled as ARD systems in the continuum limit. For example, instead of modeling the motion of a disease in a moving population using discrete network models, it might be more profitable to model the population as a flow and treat the spreading disease as a front that is propagating in this flow.

---

[1] T. Tél, A. de Moura, C. Grebogi, and G. Károlyi, "Chemical and Biological activity in open flows: A dynamical system approach," Phys. Rep. **413**, 91-196 (2005).

[2] G.A. Voth, G.H. Haller, and J.P. Gollub, "Experimental Measurements of Stretching Fields in Fluid Mixing", Phys. Rev. Lett. **88**, 254501 (2002).

[3] A.D. Kirwan, B.L. Lipphardt, Jr., A. C. Poje, L. Kantha, and M. Zweng, "25 Years of Nonlinearity in Oceanography from the Lagrangian Perspective," Nonlin. Dynam. in Geosciences, 177-196 (Springer, 2007).

[4] M.J. Olascoaga, F.J. Beron-Vera, L.E. Brand, and H. Kocak, "Tracing the early development of harmful algal blooms on the West Florida Shelf with the aid of Lagrangian coherent structures," J. Geophys. Res.—Oceans **113**, C12041 (2008).

[5] T.H. Solomon, S. Tomas and J.L. Warner, "The Role of Lobes in Chaotic Mixing of Miscible and Immiscible Impurities", Phys. Rev. Lett., **77**, 2682-2685 (1996).

[6] T.H. Solomon, S. Tomas and J.L. Warner, "Chaotic mixing of immiscible and immiscible impurities in a two-dimensional flow", Phys. Fluids **10**, 342-350 (1998).

[7] B.D. Hughes, M.F. Shlesinger and E.W. Montroll, Proc. Natl. Acad. Sci. U.S.A. **78**, 3287 (1981).

[8] E.W. Montroll and M.F. Shlesinger, in *Nonequilibrium Phenomena II: From Stochastics to Hydrodynamics*, Studies in Statistical Mechanics Vol II, edited by J.L. Lebowitz and E.W. Montroll (North-Holland, Amsterdam, 1984), p. 1.

[9] M. F. Shlesinger, G. M. Zaslavsky, and J. Klafter, Nature (London) **363**, 31 (1993).

[10] T.H. Solomon, Eric R. Weeks and Harry L. Swinney, "Observation of Anomalous Diffusion and Lévy Flights in a Two-Dimensional Rotating Flow," Phys. Rev. Lett. **71**, 3975-3978 (1993).

[11] T.H. Solomon, A.T. Lee, and M.A. Fogleman, "Resonant flights and transient superdiffusion in a time-periodic, two-dimensional flow", Physica D **157**, 40-53 (2001).

[12] M.S. Paoletti, C. R. Nugent and T.H. Solomon, "Synchronization of Oscillating Reactions in an Extended Fluid System", Phys. Rev. Lett. **96**, 124101 (2006).

[13] D. Brockmann, L. Hufnagel and T. Geisel, "The Scaling Laws of Human Travel," Nature **439**, 462-465 (2006).

[14] G. Ramos-Fernández, J. L. Mateos, O. Miramontes, G. Cocho, H. Larralde and B. Ayala-Orozco, "Lévy Walk Patterns in the Foraging Movements of Spider Monkeys (Ateles Geoffroyi)", Behav. Ecol. Sociobiol. **55**, 223-230 (2004).
[15] A.M. Reynolds, "Cooperative random Lévy flight searches and the flight patterns of honeybees", Phys. Lett. A **354**, 384-388 (2006).
[16] P. Grindrod, *The Theory and Applications of Reaction-Diffusion Equations: Patterns and Waves* (Clarendon Press, Oxford, 1996).
[17] R. J. Field and M. Burger, *Oscillations and Traveling Waves in Chemical Systems* (Wiley, New York, 1985).
[18] Y. Kuramoto, *Chemical Oscillations, Waves and Turbulence* (Springer, Berlin, 1984).
[19] M. Abel, M. Cencini, D. Vergni, and A. Vulpiani, Chaos **12**, 481 (2002).
[20] M. Cencini, A. Torcini, D. Vergni, and A. Vulpiani, Phys. Fluids **15**, 679 (2003).
[21] R. A. Fisher, Proc. Annu. Symp. Eugen. Soc. **7**, 355 (1937).
[22] A. N. Kolmogorov, I. G. Petrovskii, and N. S. Piskunov, Moscow Univ. Math. Bull. (Engl. Transl.) **1**, 1 (1937).
[23] Qu, Weiss and Garfinkel, A. J. Physiol. Heart Circ. Physiol 276, H269-H283 (1999).
[24] M.A. Dahlem and S.C. Müller, "Reaction-diffusion waves in neuronal tissue and the window of cortical excitability", Annalen der Physik **13**, 442-449 (2004).
[25] C. Van Oss, A.V. Panfilov, P. Hogeweg, F. Siegert and C.J. Weijer, "Spatial pattern formation during aggregation of the slime mould Dictyostelium discoideum", J. Theoret. Biol. **181**, 203-213 (1996).
[26] Z. Neufeld, P.H. Haynes and T. Tel, "Chaotic mixing induced transitions in reaction-diffusion systems", Chaos **12**, 426 (2002).
[27] M.E. Schwartz and T.H. Solomon, "Chemical Reaction Fronts in Ordered and Disordered Cellular Flows with Opposing Winds", Phys. Rev. Lett. **100**, 028302 (2008).
[28] G. Metcalfe and J.M. Ottino, "Autocatalytic Processes in Mixing Flows", Phys. Rev. Lett. **72**, 2875-2878 (1994).
[29] P.E. Arratia and J.P. Gollub, "Predicting the Progress of Diffusively Limited Chemical Reactions in the Presence of Chaotic Advection", Phys. Rev. Lett. **96**, 024501 (2006).
[30] C.R. Nugent, W.M. Quarles and T.H. Solomon, "Experimental studies of pattern formation in a reaction-advection-diffusion system," Phys. Rev. Lett. **93**, 218301 (2004).
[31] Y. Lehahn, F. d'Ovidio, M. Lévy and E. Heifetz, "Stirring of the northeast Atlantic spring bloom: A Lagrangian analysis based on multisatellite data", J. Geophys. Res. **112**, C08005 (2007).
[32] E. Hernández-Garcia and C. López, "Sustained plankton blooms under open chaotic flows", Ecological Complexity **1**, 253-259 (2004).
[33] S. R. Cox, "Persistent Localized states for a chaotically mixed bistable reaction," Phys. Rev. E **74**, 056206 (2006).
[34] C.S. Zhou, J. Kurths, Z. Neufeld and I.Z. Kiss Phys. Rev. Lett. **91,** 150601 (2003); **Z.** Neufeld, I.Z. Kiss, C.S. Zhou and J. Kurths, Phys. Rev. Lett. **91**, 084101 (2003).
[35] I.Z. Kiss, W. Wang, and J. L. Hudson, "Experiments on Arrays of Globally Coupled Periodic Electrochemical Oscillators", J. Phys. Chem. B **103**, 11433-11444 (1999); I.Z. Kiss, Y. Zhai and J. L. Hudson, "Emerging Coherence in a Population of Chemical Oscillators", Science **296**, 1676-1678 (2002).
[36] D.J. Watts and S.H.Strogatz, "Collective Dynamics of 'Small World' Networks", Nature **393**, 440-442 (1998).
[37] M. Tinsley, J.X. Cui, F.V. Chirila, A. Taylor, S. Zhong and K. Showalter, "Spatiotemporal Networks in Addressable Excitable Media", Phys. Rev. Lett. **95**, 038306 (2005).
[38] R. Mancinelli, D. Vergni, and A. Vulpiani, Europhys. Lett. **60**, 532 (2002); D. del Castillo-Negrete, B. A. Carreras, and V. E. Lynch, Phys. Rev. Lett. **91**, 018302 (2003); D. Brockmann and L. Hufnagel, Phys. Rev. Lett. **98**, 178301 (2007).
[39] M.S. Paoletti and T.H. Solomon, "Experimental studies of front propagation and mode-locking in an advection-reaction-diffusion system", Europhys. Lett. **69**, 819-825 (2005);M.S. Paoletti and T.H. Solomon, "Front Propagation and Mode-Locking in an Advection-Reaction-Diffusion System," Phys. Rev. E **72**, 046204 (2005).
[40] M. Sandulescu, C.E. Lopez, E. Hernandez-Garcia and U. Feudel, "Plankton blooms in vortices: the role of biological and hydrodynamics timescales", Nonlin. Processes Geophys. **14**, (2007), 443-454.